

Effect of initial resist thickness on residual layer thickness of nanoimprinted structures

Hae-Jeong Lee, Hyun Wook Ro, Christopher L. Soles,^{a)} Ronald L. Jones, Eric K. Lin, and Wen-li Wu

NIST Polymers Division, 100 Bureau Drive, Gaithersburg, Maryland 20899-8541

D. R. Hines

University of Maryland, Laboratory for Physical Sciences, 8050 Greenmead Drive, College Park, Maryland 20740

(Received 2 June 2005; accepted 6 September 2005; published 6 December 2005)

Quantification and control of the residual layer thickness is a critical challenge facing nanoimprint lithography. This thickness must be known to within a few nanometers, yet there are very few nondestructive measurement techniques capable of extracting such information. Here we describe a specular x-ray reflectivity technique that can be used to not only quantify the thickness of the residual layer with sub-nm resolution, but also to extract the pattern height, the line-to-space ratio, and relative linewidth variations as a function of the pattern height. This is illustrated through a series of imprints where the initial film thickness is varied. For films with sufficient resist material to fill the mold, complete pattern filling is observed and the residual layer thickness is directly proportional to the initial film thickness. When there is insufficient resist material in the film to completely fill the patterns in the mold, a finite residual layer thickness of approximately 50–100 Å is still observed. © 2005 American Vacuum Society. [DOI: 10.1116/1.2101776]

I. INTRODUCTION

Nanoimprint lithography (NIL) is becoming a next generation lithography of significant interest due to its low cost and a potential patterning resolution of 10 nm or less.¹ NIL entails fabricating patterns once into a hard mold or master, typically made out of Si or quartz, using a high resolution technique such as e-beam lithography. By stamping this mold into a soft resist film, usually under elevated temperature and pressure, the patterns in the master can then be rapidly duplicated. It is also possible to stamp the master at room temperature into a liquid monomer that cross-links into a rigid pattern under ultraviolet radiation. Both of these NIL variations leave a thin residual layer of resist between the features of the mold and supporting substrate, owing to the fact that the mold is unable to fully displace the resist and make direct contact with the underlying substrate. It is straightforward to remove the residual layer through a reactive ion etch (RIE) process. The RIE etch is anisotropic and biased to etch in the thickness direction, however there is always a slight lateral erosion of the feature widths. To minimize this lateral trimming one must minimize the residual layer thickness. The problem is exacerbated when there are residual layer variations across the imprint field.^{2,3} In the presence of uneven residual layers, an accelerated lateral trimming occurs where the RIE breaks through the thinnest residual layer regions first.⁴ An optimally thin and uniform residual layer is critical to minimize the lateral trimming and loss of critical dimension control in these etch processes.⁵

Optimizing the RIE processing conditions mandates a precise knowledge of the residual layer thickness. Specular

x-ray reflectivity (SXR) is well established for measuring the thickness, density, and roughness of nonpatterned thin films supported on a smooth substrate.⁶ The electron density profile perpendicular to the plane of the film can be obtained by fitting the SXR data with a multilayer recursive model based on a one-dimensional solution to the Schrödinger equation.^{6,7} In this work we extend the use of SXR to surfaces patterned by NIL where the characteristic length scales of the patterns are in the sub- μm range. In this limit the modeling of the SXR data can be used to quantify the residual layer thickness and the height of the imprinted patterns with sub-nm precision. The residual layer thickness and pattern height are quantified over a wide range for a series of imprints where the initial resist thickness ranges from excessively thick down to the limit where there is not enough resist in the film to fill the patterns in the mold. These studies illustrate the utility of SXR in developing, optimizing, and controlling NIL nanofabrication processes.

II. EXPERIMENT

A large area imprint mold with parallel lines and spaces (fabricated by interference lithography) was purchased from Nanonex (Certain commercial materials and equipment are identified in this article in order to specify adequately the experimental procedure. In no case does such identification imply recommendation by the National Institute of Standards and Technology nor does it imply that the material or equipment identified is necessarily the best available for this purpose.) The patterns in the mold were fabricated by reactive ion etching into a thick (several micrometers) silicon oxide layer on top of a 10.16-cm-(4 in.)-diam Si wafer. The mold was designed with approximately a 200 nm pitch and a line-

^{a)}Author to whom correspondence should be addressed; electronic mail: csoles@nist.gov

to-space ratio of one. A fluorinated trichlorosilane was applied to the mold to produce a low energy coating that would facilitate pattern release after imprinting. The imprints were made into the Nanonex NXR-1020 resist spun onto 10.16-cm-diam Si wafers with a native oxide coating. The resist was spun at various spin speeds and also diluted with toluene to vary the initial film thickness. After spinning, the films were annealed at 80 °C under vacuum for 30 min to remove the casting solvent. The resulting films varied in thickness from 438 to 3893 Å. The imprints were made on a Nanonex NX-2000 tool. After sufficiently evacuating the sample chamber, imprints were made in two steps: 10 s at 130 °C and 1.4 MPa followed by 60 s at 130 °C and 1.7 MPa. The tool was cooled to 55 °C, below the estimated glass transition temperature of the resist, before releasing the pressure and separating the pattern from the mold.

SXR measurements were performed on a Phillips X'pert diffractometer with a θ - 2θ configuration at ambient temperature. A beam of Cu K_α radiation, $\lambda = 1.5412$ Å, was directed with a focusing mirror through a four-bounce Ge (220) crystal monochromator onto the patterned film of interest. The reflected beam was collected through a three bounce channel-cut Ge (220) crystal and directed into the solid-state detector. The goniometer has an angular reproducibility of $\pm 0.0001^\circ$. For all of the reflectivity data presented here, the mold and the imprinted pattern were oriented with their gratings perpendicular to the plane defined by the surface normal and the incident beam. The parallel orientation produced very similar results so only the perpendicular configuration is reported here.

III. RESULTS AND DISCUSSION

The SXR data are presented as $\log(R)$ vs Q where $Q = 4\pi/\lambda \sin(\theta)$, θ is the angle of incidence/reflection and λ is the x-ray wavelength. The ratio of the reflected to the incident intensities defines the reflectivity R . At small θ , there is total reflection of the incident x rays and $\log(R) = 0$. As the angle of incidence increases a critical angle θ_c is observed where $\log(R)$ becomes less than zero; this corresponds to a critical scattering vector Q_c . The magnitude of Q_c^2 is the scattering length density and is proportional to the average electron density ρ_e through the expression $Q_c^2 = 16\pi r_o \rho_e$ where r_o is the classical radius of an electron. If the atomic composition of the material is known, ρ_e can be transformed to the mass density ρ . The atomic composition of the NXR-1020 resist is not known, so the value of Q_c^2 will be used as the indication of density ($Q_c^2 \propto \rho$).

The experimental reflectivity data for the silicon oxide mold is shown in Fig. 1(a) along with the theoretical reflectivity curve for an infinitely thick smooth Si wafer. Notice the periodic Kiessig or interference fringes in the experimental data in contrast to the smooth Fresnel decay of $\log(R)$ with Q from the smooth Si surface. Kiessig fringes indicate a film where there is an appreciable electron density difference between the film and the substrate. This is striking because the mold is a *single* material of a *single* density. There are also *two* critical angles at low Q , indicated with the vertical

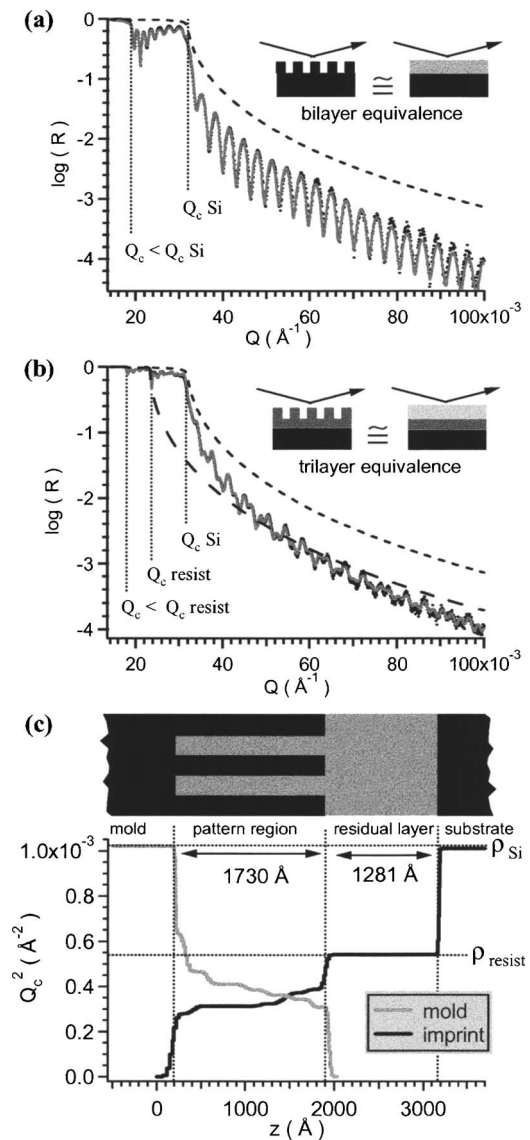


FIG. 1. Part (a) shows the reflectivity for the imprint mold (dots) and a smooth silicon wafer (short dashed line) while part (b) shows the experimental reflectivity data, the imprinted pattern (dots), the smooth silicon wafer (short dashed line), and a smooth resist film (long dashed line). The insets to parts (a) and (b) indicate the equivalent models used to model the reflectivity, while the solid gray lines through the data points indicate the fits to the model. The resulting scattering length density profiles obtained from the model fitting are displayed in part (c) for the mold (gray line) and the imprint (black line). The schematic at the top of part (c) helps orient the scattering length density profiles relative to the physical structures. The standard uncertainty in the experimental reflectivity is equal to the linewidth.

dotted lines. By contrast the smooth Si curve displays a single critical angle at $Q_{c,Si}$. The two critical angles in the patterned mold further suggest a smooth film of a density that is different from the substrate. That the second critical angle coincides with $Q_{c,Si}$ while the first critical angle occurs at $Q_c < Q_{c,Si}$ means that the apparent film on the Si substrate has a density less than Si. Technically the patterns in the mold are fabricated into silicon oxide, not Si. In practice there is a small difference in the Q_c values of Si and silicon oxide. However, the exact Q_c for the oxide varies somewhat

depending on the density of the oxide. For this reason the mold and the supporting substrate are simplified as pure Si. The effect of this assumption on the results presented here is negligible.

The most logical way these observations can be rationalized is illustrated in the inset of Fig. 1(a). SXR must average density over lateral length scales that are larger than periodicity of the patterns. This leads to the “bilayer equivalency” where the patterned region, comprised of Si lines and empty spaces between the lines, can be modeled as a homogenous layer with a density that is a rule of mixtures average of the volume of Si in the lines and the volume of air in the gaps. This same density averaging concept is the basis for SXR measurements of the density and porosity of nanoporous low dielectric constant materials.⁸ The solid line in Fig. 1(a) is a fit using the equivalent bilayer model, showing excellent agreement with the experimental data.⁷

The SXR data from one of the imprints in Fig. 1(b) also shows Kiessig fringes, but they are less regular and show a beating of multiple periodicities that would be indicative of a multilayer. Likewise, the three vertical dotted lines indicate a series of three critical angles. This suggests the multilayer is comprised of three different densities. As in Fig. 1(a), the largest critical angle coincides with $Q_{c, Si}$, consistent with the supporting Si substrate. Figure 1(b) also shows the theoretical reflectivity from a smooth resist film. The intermediate critical angle coincides with the critical angle for the resist, $Q_{c, resist}$, while the first critical angle occurs at $Q_c < Q_{c, resist}$. The most probable physical model to describe this scenario is indicated schematically in the inset of Fig. 1(b) in terms of a trilayer equivalent model. The reflectivity can be modeled with a Si substrate, an intermediate residual layer of resist, and a top patterned layer that has a density of the resist reduced by the appropriate rule of mixtures for the volume of material in the line relative to the spaces. The solid line in Fig. 1(b) indicates the best fit of this model to the experimental data.

The physical models corresponding to the best fits in Figs. 1(a) and 1(b) are shown in part (c) in terms of Q_c^2 plotted as a function of distance z through the film. The horizontal axis has been assigned with $z=0$ Å nominally corresponding to the bottom of the trenches in the mold, with z increasing with distance toward the top of the mold patterns. A schematic at the top of Fig. 1(c) is provided to help correlate the Q_c^2 profiles with a physical model of the mold and imprint. At $z=0$, Q_c^2 jumps immediately from $1.02 \pm 0.05 \times 10^{-3} \text{ \AA}^{-2}$ (the value for pure Si) down to $0.635 \pm 0.05 \times 10^{-3} \text{ \AA}^{-2}$ in the region which corresponds to the bottom of the trenches in line/space patterns of the mold.⁹ As z continues to increase, Q_c^2 decreases gradually from $0.635 \pm 0.05 \times 10^{-3} \text{ \AA}^{-2}$ down to $0.309 \pm 0.05 \times 10^{-3} \text{ \AA}^{-2}$ over the next 1730 ± 10 Å before abruptly dropping to zero. This means that the pattern height (or gap depth) in the mold is 1730 ± 10 Å.

As mentioned above, these profiles are fit by building up multilayer models. The simplified cartoon in Fig. 1(a) implies that two layers are needed to fit the reflectivity for the mold. In reality, eight layers were needed including one for the Si substrate and seven for the patterned region. These seven layers are evident in Fig. 1(c) through the discrete changes of Q_c^2 from $0.635 \pm 0.05 \times 10^{-3} \text{ \AA}^{-2}$ to $0.309 \pm 0.05 \times 10^{-3} \text{ \AA}^{-2}$ over the 1730 ± 10 Å that represent the pattern height. This discretization is a limitation of the multilayer modeling software and it is emphasized that a smooth and continuous profile is physically appropriate. Nevertheless, SXR can be used to accurately quantify the pattern height. It should also be pointed out that at any position z along the profile, the relative values of Q_c^2 for the fully dense Si and patterned region give the line-to-space ratio. For example, at the bottom of the mold trench the line-to-space ratio is $0.635/(1.02-0.635)=1.6$. This line-to-space ratio is, however, only relative; SXR alone does not provide information on the absolute line or space width.

The Q_c^2 profile for the imprinted pattern is also shown in Fig. 1(c) (black line) with $z=0$ Å nominally coinciding with the tops of the resist patterns that would mate with the bottom of the mold gaps and z increases with distance away from the mold. This illustrates how the patterns in the mold mate with the patterns in the imprint. Q_c^2 starts at $0.279 \pm 0.05 \times 10^{-3} \text{ \AA}^{-2}$ at the top of the resist patterns and gently increases to $0.389 \pm 0.05 \times 10^{-3} \text{ \AA}^{-2}$ over the next 1720 ± 10 Å before rapidly increasing to $0.542 \pm 0.05 \times 10^{-3} \text{ \AA}^{-2}$, the Q_c^2 of the fully dense or pure resist. As z continues to increase, Q_c^2 remains constant for the next 1281 ± 10 Å before increasing abruptly to $1.02 \pm 0.05 \times 10^{-3} \text{ \AA}^{-2}$ at the resist/Si interface. From these profiles it can be deduced that the residual layer thickness is 1281 ± 10 Å and the resist pattern height is 1720 ± 10 Å. The resist pattern height is in excellent agreement with the 1730 ± 10 Å depth of the trenches in the mold, indicating that the resist material completely filled the mold during the imprint.

We now apply these measurements to a series of imprints in which the initial resist thickness (before imprinting) is varied from 438 ± 10 to 3893 ± 10 Å. The initial thickness for the imprint in Fig. 1 was 2217 ± 10 Å. The SXR curves for a few of these imprints are displayed in Fig. 2. As in Fig. 1(b), the three vertical dotted lines indicate the three Q_c s. As the initial film thickness decreases, the interference fringes grow in wavelength due to the inverse proportionality of the periodicity to the total film thickness. Notice that the strength of the critical angle at the intermediate Q_c related to the residual layer becomes less pronounced as the film thickness decreases. This is because there is less x-ray absorption in thinner films for this so-called wave-guiding region. This intermediate critical angle becomes almost indistinguishable when the initial film thickness is less than 1328 Å. On the contrary, the strength of the first critical angle, related to the patterned layer, does not change with film thickness until the thinnest film is reached. This suggests that the pattern height does not change significantly, unlike the residual layer, until

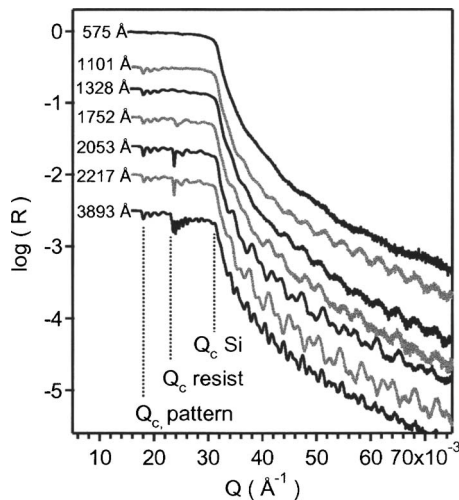


FIG. 2. Experimental x-ray reflectivity data are shown for imprints where the initial resist thickness varied from 3893 to 575 Å. The exact thickness is indicated to the left of each curve. The standard uncertainty in the experimental reflectivity is equal to the linewidth.

the initial film thickness drops below nominally 1000 Å. For the thinnest initial film thickness shown in Fig. 2 (575 Å), the features in the reflectivity curves become highly deteriorated, probably reflecting poorly defined patterns.

The Q_c^2 profiles obtained by fitting these reflectivity curves are shown in Fig. 3. Consistent with Fig. 1(c), the origin of the abscissa is assigned to the top of the pattern and z increases with distance into the pattern towards the supporting Si substrate. Plotted this way it is clear that pattern height does not vary significantly in most of the imprints. The only exceptions are the two thinnest films, which display reduced pattern heights. By contrast there is a significant variation of the residual layer thickness in the initial thickness of the resist film. Figure 4 helps quantify these relationships between the initial resist thickness and both the pattern height and the thickness of residual layers. In Fig. 4 it is clear that the pattern height remains constant at approximately 1720 Å as long as the initial thickness is greater than approximately 1000 Å; for all films thicker than 1000 Å the resist material is able to completely fill the mold under applied imprint conditions. For these same films the residual

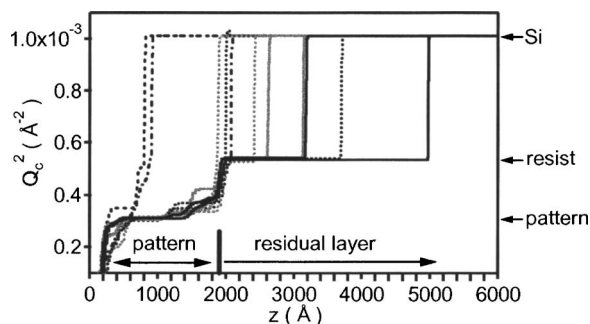


FIG. 3. Scattering length density profile is displayed as a function of distance for several imprints as function of the initial film thickness. These profiles are derived from the best fit to the experimental data in Fig. 2 using a multilayer fitting routine (see Ref. 7).

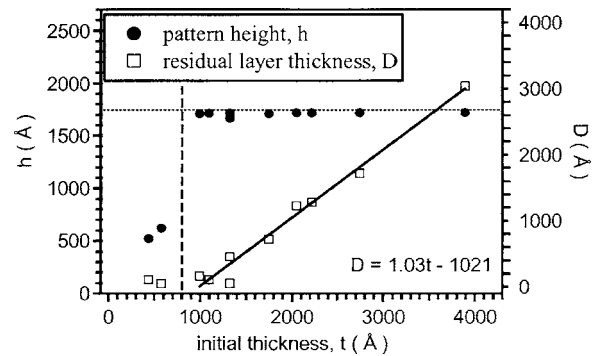


FIG. 4. Variations of the imprint pattern height and the residual layer thickness are displayed as a function of initial resist thickness. The straight solid line is a linear fit with a slope of nearly unity, indicating direct proportionality between the residual layer thickness and the initial film thickness as long as there is enough material to completely fill the mold. For data points to the left of the solid dashed line there is insufficient material in the resist film to completely fill the mold. The horizontal dotted line indicates the height of the gaps in the mold that the resist material flows into. The standard uncertainty in the residual layer thickness and the pattern height is equal to the size of the data points.

layer thickness decreases in direct proportion (proportionality of unity) to the initial film thickness, as would be expected for a volume conserving imprint process. The vertical dashed line in Fig. 4 indicates the initial film thickness when there would be exactly enough resist material in the film to completely fill the mold. As expected, the two imprints where the initial film thickness is less than this volume filling mark lead to incomplete mold fill. However, these two films also display a finite residual layer of 50–100 Å. Even though there is still resist material within the residual layer to potentially fill the pattern, its flow into the mold is constrained. The residual layer thickness appears to plateau in the 50–100 Å range when the initial film thickness drops below 1000 Å.

It is generally believed that conventional imprinting processes cannot avoid a finite residual layer. The findings presented here support this notion, although variations in the imprint pressure, temperature, or resist formulations were not explored. A finite residual layer is consistent with surface forces apparatus measurements of simple liquids, both small molecule and polymeric, confined between mica surfaces.^{10–12} These measurements show that the shear relaxation time and effective viscosity of the liquid film increase strongly when the thickness of the film approaches approximately ten molecular diameters. This length scale is commensurate with the 50–100 Å plateau in the residual layer thickness reported here. In some cases, this increased viscosity of the liquid film with decreasing separation has been likened to an induced liquid-to-glass transition.¹² Such an increase in viscosity is consistent with the observation that when the mold approaches the substrate to within a few molecular diameters of the resist, the lateral flow of the resist is restrained. There is often the notion that the residual layer acts as a soft “cushion” to protect the mold from being dam-

aged by the substrate. In truth this cushion may become more rigid and glass-like as the residual layer thickness approaches 100 Å.

IV. CONCLUSIONS

Specular x-ray reflectivity is developed as a powerful metrology to quantify the pattern height, residual layer thickness, and relative line-to-space ratio as a function of pattern height, all with sub-nm precision, for large area periodic patterns fabricated by nanoimprint lithography. Using this technique we demonstrate an excellent fidelity of pattern transfer, with complete mold filling, for a range of imprints where the initial film thickness was greater than 1000 Å. As expected by volume filling arguments, the residual layer thickness was directly proportional to the initial film thickness. However, for films thinner than 1000 Å we found there was always a minimum residual layer of approximately 50–100 Å. This minimum residual layer thickness appears to be consistent with a layer of resist with enhanced viscosity near the supporting substrate.

ACKNOWLEDGMENTS

The authors acknowledge the financial support from the NIST Office of Microelectronics and the ATP Intramural Funding Program and the Nanonex Corporation for their assistance in fabricating the imprint patterns.

- ¹S. Y. Chou and P. R. Krauss, *Microelectron. Eng.* **35**, 237 (1997).
- ²C. Gourgon, C. Peret, G. Micouin, F. Lazzarino, J. H. Tortai, O. Jorbert, and J.-P. E. Grolier, *J. Vac. Sci. Technol. B* **21**, 98 (2003).
- ³H. Schulz, M. Wissen, and H.-C. Scheer, *Microelectron. Eng.* **67-68**, 657 (2003).
- ⁴C. Perret, C. Gourgon, G. Micouin, and J.-P. Grolier, *Jpn. J. Appl. Phys., Part 1* **41**, 4203 (2002).
- ⁵H. Lee and G. Y. Jung, *Jpn. J. Appl. Phys., Part 1* **43**, 8369 (2004).
- ⁶L. G. Parrat, *Phys. Rev.* **95**, 359 (1954).
- ⁷J. F. Ankner and C. J. Majkrzak, *Proc. SPIE* **1738**, 260 (1992).
- ⁸H. J. Lee, C. L. Soles, D. W. Liu, B. J. Bauer, E. K. Lin, W. L. Wu, and A. Grill, *J. Appl. Phys.* **95**, 2355 (2004).
- ⁹The data throughout the manuscript are presented along with standard uncertainty (\pm) involved in the measurement based on one standard deviation.
- ¹⁰R. G. Horn and J. N. Israelachvili, *Macromolecules* **21**, 2836 (1988).
- ¹¹S. Granick, *Science* **253**, 1374 (1991).
- ¹²A. Levent Demirel and S. Granick, *Phys. Rev. Lett.* **77**, 2261 (1996).